A PHANTOM STUDY OF FACTORS AFFECTING STANDARDIZED UPTAKE VALUE (SUV) MEASUREMENT OF QUANTITATIVE TC-99M MDP BONE SPECT/CT

Thinn Thinn Myint[1,2], Tawatchai Ekjeen[1], Kanyalak Wiyaporn[1], Anucha Chaichana[1], Yudthaphon Vichianin[1], Ruentip Tipparoj[3], Thonnapong Thongpraparn[3], Sunanta Chiewvit[3]

[1]Department of Radiological Technology, Faculty of Medical Technology, Mahidol University, Bangkok, Thailand
[2]Department of Nuclear Medicine, Cyclotron and PET/CT center, Yangon General Hospital, Myanmar
[3]Division of Nuclear Medicine, Department of Radiology, Faculty of Medicine Siriraj Hospital, Bangkok, Thailand

ABSTRACT

The objective was to study factors that affect standardized uptake value (SUV) measurement of quantitative ^{99m}Tc-MDP bone SPECT/CT using phantom. A cylindrical phantom was used to determine a calibration factor and a NEMA body phantom was used to measure SUV. ^{99m}Tc solution with activity of 16.38 kBq/ml was filled in the cylindrical phantom and background activity of ^{99m}Tc in the NEMA phantom with TBR of 7:1 was 18 kBq/ml. SPECT/CT data were acquired based on clinical protocol and 3D images were reconstructed using OS-EM algorithm with compensation for degrading factors. Both SUVs including SUV_{mean} and SUV_{max} were measured using Q.Metrix software and the effect of iterative update and sphere size on SUVs were investigated. The study showed that increasing iterative updates resulted in increasing both SUVs for all spheres and %differences of measured SUVs comparing with true SUV for all spheres tended to increase when sphere size decreased due to PVE.

Keywords: Phantom study, SUV, ^{99m}Tc-MDP, SPECT/CT

1. INTRODUCTION

Nowadays, activity quantification in nuclear medicine is increasingly used for a variety of clinical applications including dosimetry, diagnosis and monitoring tumor response to therapy. In quantitative single photon emission computed tomography/computed tomography (SPECT/CT) imaging, several published clinical studies have reported the use of quantitative value such as standardized uptake value (SUV) for ^{99m}Tc-MDP bone SPECT/CT and have shown to be useful for evaluation of bone disease and normal bone [1-4].

Manuscript received on May 29, 2019; revised on June 9, 2019.
*Corresponding author E mail: tawatchai.ekj@mahidol.edu Department of Radiological Technology, Faculty of Medical Technology, Mahidol University, Thailand.

To measure SUV, a calibration factor is needed in order to convert counts in voxels of the reconstructed images into radioactivity per volume (i.e., kBq/ml), which is called tissue concentration. Thus, SUV is possible to measure by normalizing tissue concentration measured in volume of interest (VOI) with injected radioactivity and patient body weight or body surface area.

Quantitative data require quantification of organ or tumor activities in nuclear medicine images. However, there are several factors that affect reliability of quantitative data of the images and these factors include physical factors, parameters for imaging protocol and image reconstruction, biology and physiology of patient [5]. The physical factors that are attenuation, scatter, collimator-detector response (CDR), and partial volume effect (PVE) must be addressed in order to achieve reliable results and iterative reconstruction is the most commonly used method for compensating these physical factors.

The aim of this study was to study the factors that affect the measurement of SUVs including mean SUV (SUV_{mean}) and maximum SUV (SUV_{max}) on quantitative ^{99m}Tc-MDP bone SPECT/CT. The number of iterative updates of OS-EM algorithm with compensation for attenuation, scatter, and resolution recovery, and sphere sizes on SUVs were investigated using a NEMA body phantom.

2. MATERIALS AND METHODS

2.1. Measurement of tumor to background ratio (TBR) from clinical data

It is essential to simulate the sphere of the NEMA body phantom similar to tumor found in clinical data. In this study, tumor to background ratio (TBR) was measured from 35 retrospective data (92 bone lesions) of ^{99m}Tc-MDP bone SPECT/CT studies and the data collection process was approved by local ethic committee. To measure TBR, the SPECT data were reconstructed using 3D OS-EM algorithm with 2 iterations and 10 subsets. In the reconstruction, compensations for attenuation, scatter and resolution recovery without post-reconstruction filtering were used and all reconstruction parameters were based on clinical protocol.

After obtaining the quantitative reconstructed SPECT images, volume of interest (VOI) was drawn around each abnormal bone lesion in the transaxial SPECT images and total counts in the VOI were measured. This VOI was then copied to normal bone and background area in the same slice as bone lesion was presented. After that, total counts for normal bone and background area were measured and thus, TBR was calculated as follows [6]:

$$\mathrm{TBR} = \frac{\text{Abnormal lesion counts - Background counts}}{\text{Normal bone counts - Background counts}} \quad (1)$$

In this study, the average TBR that was measured from 92 lesions of bone metastasis was 7.01 ± 5.86 (average ± SD) and this TBR was used to set the contrast of hot spheres in the NEMA body phantom.

2.2. Determination of calibration factor

A large cylindrical phantom with a diameter of 20 cm, height of 22 cm, weight of 7.6 kg, and a total volume of 5,500 ml as shown in Figure 1, was used to measure a calibration factor. The phantom was filled with ^{99m}Tc solution with activity concentration of 16.38 kBq/ml. The projection data were acquired using GE Discovery NM/CT 670 Pro SPECT/CT system with LEHR collimator based on clinical routine protocol of ^{99m}Tc-MDP bone SPECT/CT imaging at Division of Nuclear Medicine, Siriraj hospital.

Figure 1. A large cylindrical phantom.

For ^{99m}Tc-MDP bone SPECT/CT protocol, the emission data were firstly acquired using step-and-shoot data acquisition with 60 projections over 360-degree, 15 seconds per step, 6-degree angular step, non-circular orbit, and matrix size of 128 × 128. For energy setting, the photopeak window was set at 140 keV with 20% window width and the scatter window was set at 120 keV with 10% window width. After that, CT scan of the phantom was performed using tube voltage of 140 kVp and Smart mA. The slice thickness was 2.5 mm and matrix size was 512 × 512.

The projection data were reconstructed using 3D OS-EM algorithm with 2 iterations and 10 subsets. The data were corrected for CT-based attenuation correction and dual-energy window-based scatter correction without post-reconstruction filtering. To measure calibration factor, a large VOI, V_{vol}, was drawn in the reconstructed images for the whole volume of the cylindrical phantom and total counts for a large VOI, C_{vol}, were measured. The calibration factor (CF) was then calculated as follows [7]:

$$\mathrm{CF} = \frac{R}{V_{vol} \cdot C_{vol}} \times \exp\left(\frac{T_0 - T_{cal}}{T_{1/2}} \ln 2\right) \times \left(\frac{T_{acq}}{T_{1/2}} \ln 2\right) \times \left(1 - \exp\left(-\frac{T_{acq}}{T_{1/2}} \ln 2\right)\right)^{-1} \quad (2)$$

where R is the counting rate derived from the reconstructed image (counts/dwell time) and measured in VOI. T_0 is the start time of acquisition, T_{cal} is the time of the activity calibration, $T_{1/2}$ is the half-life of the radioisotope, and T_{acq} is the time duration of the acquisition. In this study, the calculated calibration factor was 4.92 cps/kBq. This calibration factor was used later for SUV measurement.

2.3. A phantom study

2.3.1 Phantom preparation

A NEMA body phantom, which consists of a torso cavity, and six spheres with inner diameters of 10, 13, 17, 22, 28 and 37 mm was used as shown in Figure 2. The phantom mimics the shape of an upper human body with 24.1 × 30.5 × 24.1 cm (height × width × depth). The total volume of this phantom is 10,012 ml and the weight is 10.1 kg without lung insert. To mimic tumor, each sphere was filled with ^{99m}Tc solution and TBR of 7:1 was studied according to retrospective patient data. In addition, activity concentration level in the background of the phantom was 18 kBq/ml, which was obtained from published clinical study of ^{99m}Tc-MDP bone SPECT/CT imaging [8].

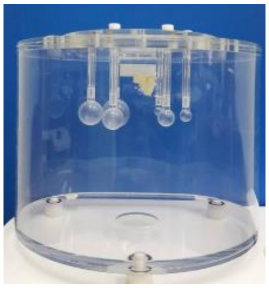

Figure 2. A NEMA body phantom with six spheres varying in sizes.

2.3.2 Data acquisition and image reconstruction

SPECT/CT imaging of NEMA phantom was performed for three times based on clinical protocol as mentioned previously. To obtain quantitative data, SPECT data were reconstructed using 3D OS-EM algorithm with compensation for attenuation, scatter and resolution recovery. In this study, the number of iterative update of the OS-EM algorithm was investigated by varying the number of iterations from 1 to 5 with 10 subsets. The reconstructed images for each iterative update was then post-filtered using Butterworth filter with cut-off frequency of 0.48 cycle/cm and order of 10.

2.3.3 Measurement of standardized uptake value (SUV)

Commercially available Q.Matrix software was used to measure SUVs including SUV_{mean} and SUV_{max}. The transaxial images for both SPECT and CT were used in the software. In addition, the software required calibration factor, patient and radiotracer information. To measure SUV, the VOI was drawn semi-automatically for each sphere of the phantom based on the low-dose CT images. We carefully drawn the VOI to cover the entire volume of the sphere. Finally, SUVs for each sphere were measured. According to the triple data acquisition, average values of SUV_{mean} and SUV_{max} for each iterative update and sphere size were calculated.

2.4. Data analysis

For each sphere, the measured SUVs of each iterative update of the OS-EM algorithm were compared with true SUV (SUV_{true}), which was 7.06 g/ml, and the percentage of difference (%difference) was calculated as follows:

$$\%\text{Difference} = \frac{SUV_{true} - SUV_{measured}}{SUV_{true}} \times 100 \qquad (3)$$

3. RESULTS

The results of the phantom study with TBR of 7:1 showed that the smallest sphere size that could be detected was 13 mm. Thus, both SUVs (SUV_{mean} and SUV_{max}) were measured for five spheres from 13 mm to 37 mm. For the effect of iterative update of OS-EM algorithm, plots of SUV_{mean} and SUV_{max} as a function of iterative update are shown in Figure 3 and the results showed that both SUVs for all sphere sizes increased when the number of iterative updates increased from 10 to 50.

When comparing with SUV_{true}, %differences of SUV_{mean} and SUV_{max} of each sphere for each iterative update are shown in Table 1 and Table 2, respectively. For all iterative updates, SUV_{mean} provided underestimated values for all 5 spheres. The %difference of SUV_{mean} decreased when the number of iterative update increased and the highest of %difference was found for the smallest sphere size.

Similarly, for all iterative updates, underestimation of SUV_{max} were found for the 4 spheres from 13 mm to 28 mm. However, for the largest sphere of 37 mm, underestimated values were found at 10 iterative updates while the other updates from 20 to 50 updates provided overestimation of SUV_{max}.

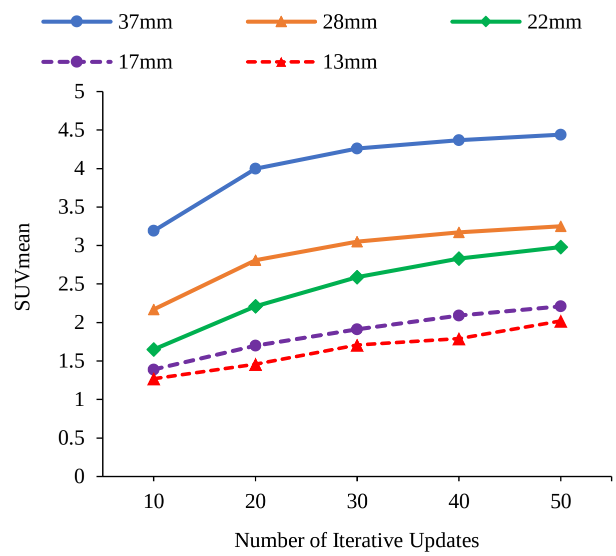

(A)

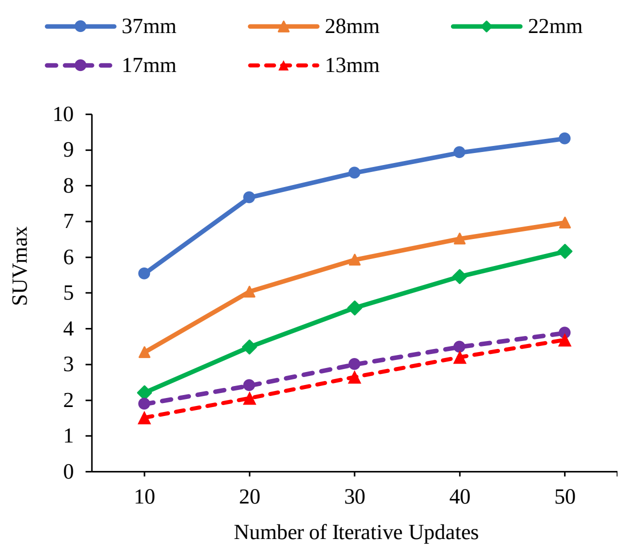

(B)

Figure 3. Plots of SUV_{mean} (A) and SUV_{max} (B) as a function of iteration update for all spheres with TBR of 7:1.

Table 1. The percentage of difference (%difference) of SUV_{mean} with a number of iterative update.

Iterative Update	%Difference of SUV_{mean}				
	Sphere Size (mm)				
	37	28	22	17	13
10	-54.83	-69.27	-76.63	-80.32	-82.02
20	-43.36	-60.29	-68.70	-75.93	-79.33
30	-39.67	-56.81	-63.32	-72.95	-75.78
40	-38.16	-55.11	-59.92	-70.40	-74.65
50	-37.12	-53.98	-57.80	-68.70	-71.39

Table 2. The percentage of difference (%difference) of SUV_{max} with a number of iterative update.

Iterative Update	%Difference of SUV_{max}				
	Sphere Size (mm)				
	37	28	22	17	13
10	-21.55	-52.70	-68.70	-73.23	-78.57
20	8.61	-28.63	-50.58	-65.87	-70.83
30	18.39	-16.02	-35.14	-57.52	-62.47
40	26.46	-7.67	-22.68	-50.58	-54.68
50	31.98	-1.30	-12.77	-45.05	-47.74

4. DISCUSSION

SPECT data are affected by several physical factors such as photon attenuation, scatter, collimator-detector response, and partial volume effect [5]. Reliability of quantification in SPECT can be achieved by compensating all of these factors via the use of iterative reconstruction (IR)-based compensation. Several publications have reported the use of IR-based compensation to improve image quality and quantitative accuracy [9-13]. The OS-EM is often the IR algorithm of choice and commonly used in clinic. For this reason, this study used OS-EM algorithm with compensations for attenuation, scatter, and resolution recovery in order to achieve quantitative data.

Another requirement for absolute quantification is a calibration factor, which is used for converting counts of the reconstructed images into concentration of radioactivity. In this study, the calibration factor was obtained by using a large cylindrical phantom, which was similar to several published studies [13, 14]. This phantom is recommended in order to avoid partial volume effect. In addition, An et al. [15] reported that inaccuracy of measured activity was reduced when the calibration factor using a uniform cylindrical phantom was applied comparing with a Petri dish.

To study factors affecting SUVs, the NEMA body phantom with TBR of 7:1, which was obtained from clinical patient data, was studied and we found that the sphere size with diameter of 10 mm was undetected and this result was similar to several published studies [8, 16]. However, other five spheres (13 mm to 37 mm) were visible and used to measure SUV_{mean} and SUV_{max}. For the effect of number of iterative update, the OS-EM algorithm with 10 subsets was used and iterative update was varied from 10 to 50 updates. The result showed that when iterative update increased, SUV_{mean} and SUV_{max} also increased. The results of this study were similar to several published PET studies, which mentioned that SUV tended to increase when the iterative update increased [17, 18].

For the effect of sphere size, %differences of measured SUVs comparing with true SUV increased for smaller spheres. Similarly, Nakahara et al. [8] showed that all SUVs (SUV_{mean}, SUV_{max}, and SUV_{peak}) tended to decrease when sphere size decreased for all four SPECT/CT system. Moreover, Baily et al. [12] studied SUV measurement in SPECT using IEC phantom with TBR of 8.2 and reported that %difference of SUV was increased for smaller spheres.

The reason for underestimation of SUV as reported in this study is due to partial volume effect (PVE) that arises from the finite spatial resolution of the imaging system. The PVE can strongly affect qualitative and quantitative measurements. For any hot tumor with a small size, the maximum value in the hot tumor will be lower than the actual value [20]. To reduce this effect, the correction for PVE must be applied. Several methods for PVE correction have been proposed and a review of partial volume correction techniques for emission tomography can be found in Erlandsson et al. [21]. Recovery coefficient (RC) is a simple method for PVE correction and is defined as the measured activity concentration of an object divided by its true concentration. The RC-based correction for PVE will be applied in the future study in order to achieve accurate SUV.

5. CONCLUSION

A large cylindrical phantom was used in this study to measure a calibration factor, which was used for converting counts in the images into activity concentration. For factors affecting SUVs (SUV_{mean} and SUV_{max}), the number of iterative update of the OS-EM algorithm with compensation for physical factors and sphere size were investigated using a NEMA body phantom. For TBR of 7:1, five sphere sizes from 13 mm to 37 mm could be detected while the smallest sphere of 10 mm was undetected. When the iterative update increased, both measured SUVs increased. The smallest sphere size provided the highest %difference of SUVs and PVE played an important role for this effect.

6. ACKNOWLEDGEMENT

The authors would like to thank Division of Nuclear Medicine, Department of Radiology, Siriraj Hospital and Department of Radiological Technology, Faculty of Medical Technology, Mahidol University for supporting all facilities.

REFERENCES

[1] M.S. Suh, W.W. Lee, Y.K. Kim, P. Yun, and S.E. Kim, "Maximum standardized uptake value of ^{99m}Tc hydroxymethylene diphosphonate SPECT/CT for the evaluation of temporpmandibular joint disorder," *Radiology*, vol. 280, pp. 890-896, 2016.

[2] T. Kaneta, M. Ogawa, H. Daisaki, S. Nawata, K. Yoshida, and T. Inoue, "SUV measurement of normal vertebrae using SPECT/CT with Tc-99m methylene diphosphonate," *Am. J. Nucl. Med. Mol. Imaging*, vol. 6, pp.262-268, 2016.

[3] R. Wang, X. Duan, C. Shen, D. Han, J. Ma, H. Wu, et al., "A retrospective study of SPECT/CT scans using SUV measurement of the normal pelvis with Tc-99m methylene diphosphonate," *Int. J. Radiol. Radiat. Oncol.*, vol. 4, pp. 3-8, 2018.

[4] I. Kuji, T. Yamane, A. Seto, Y. Yasumizu, S. Shirotake, and M. Oyama, "Skeletal standardized uptake values obtained by quantitative SPECT/CT as an osteoblastic biomarker for the discrimination of active bone metastasis in prostate cancer," *European Journal of Hybrid Imaging*, vol. 1, pp. 1-16, 2017.

[5] E.C. Frey, J.L. Humm, and M. Ljungberg, "Accuracy and precision of radioactivity quantification in nuclear medicine images," *Semin. Nucl. Med.*, vol. 42, pp. 208-218, 2012.

[6] B.D.F. Lopez, and S.C.M. Corral, "Comparison of planar bone scintigraphy and single photon emission computed tomography for diagnosis of active condylar hyperplasia," *Journal of cranio-maxillo-facial surgery*, vol. 44, pp. 70-74, 2016.

[7] P. Ritt, H. Vija, J. Hornegger, and T. Kuwert, "Absolute quantification in SPECT," *Eur. J. Nucl. Med. Mol. Imaging*, vol. 38, pp. 69-77, 2011.

[8] T. Nakahara, H. Daisaki, Y. Yamamoto, T. Iimori, K. Miyagawa, T. Okamoto, et al., "Use of a digital phantom developed by QIBA for harmonizing SUVs obtained from the state-of-the-art SPECT/CT systems: a multicenter study," *EJNMMI Research*, vol. 7, pp. 53, 2017.

[9] T. Ekjeen, C. Tocharoenchai, P. Pusuwan, and E.C. Frey, "A comparison of dual-tracer Tc-99m pertechnetate and Tc-99m MIBI with and without subtraction SPECT in the detection of abnormal parathyroid gland," *International Journal of Applied Biomedical Engineering*, vol. 11, pp. 21-26, 2018.

[10] E.C. Frey, K.L. Gilland, and B.M.W. Tsui, "Application of task-based measures of image quality to optimization and evaluation of three-dimensional reconstruction-based compensation methods in myocardial perfusion SPECT," *IEEE Trans. Med. Im.*, vol. 21, pp.1040-1050, 2002.

[11] F. Dong, L. Li, Y. Bian, G. Li, X. Han, M. Li, et al., "Standardized uptake value using thyroid quantitative SPECT/CT for the diagnosis and evaluation of Graves' disease: a prospective multicenter study," *BioMed Research International*, pp. 1-88, 2019.

[12] DL. Baily, and K.P. Willowson, "An evidence-based review of quantitative SPECT imaging and potential clinical applications," *J. Nucl. Med.*, vol. 54, pp. 83-89, 2013.

[13] J. Zeintl, A.H. Vija, A. Yahil, J. Hornegger, and T. Kuwert, "Quantitative accuracy of clinical ^{99m}Tc SPECT/CT using ordered-subset expectation maximization with 3-dimensional resolution recovery, attenuation, and scatter correction," *J. Nucl. Med.*, vol. 51, pp. 921-928, 2010.

[14] I.S. Armstrong, and S.A. Hoffmann, "Activity concentration measurements using a conjugate gradient (Siemens xSPECT) reconstruction algorithm in SPECT/CT," *Nuclear Medicine Communications*, vol. 37, pp. 1212-1217, 2016.

[15] H.J. An, M.S. Lee, and J.S. Lee, "Feasibility study of simple SPECT/CT system sensitivity measurement for ^{131}I absolute quantification," *J. Nucl. Med.*, vol. 57 (supplement 2), pp. 1880, 2016.

[16] A. Collarino, L.M.P. Arias-Bouda, R.A.V. Olmos, P. van der Tol, P. Dibbets-Schneider, L.F. de Geus-Oei, et al., "Experimental validation of absolute SPECT/CT quantification for response monitoring in breast cancer," *Med. Phys.*, vol. 45, pp. 2143-2153, 2018.

[17] K. Wiyaporn, C. Tocharoenchai, P. Pusuwan, T. Ekjeen, S. Leaungwutiwong, and S. Thanyarak, "Factors affecting standardized uptake value (SUV) of positron emission tomography (PET) imaging with ^{18}F-FDG," *J. Med. Assoc. Thai.*, Vol. 93, pp. 108-114, 2010.

[18] M. Ivanovic, W.H. McCartney, and A. Khandani, "Standard uptake values in whole-body FDG PET: effects of acquisition and processing parameters," *IEEE Nuclear Science Symposium Conference Record*, pp. 2813-2816, 2003.

[19] C.J. Jaskowiak, J.A. Bianco, S.B. Perlman, and J.P. Fine, " Influence of reconstruction iterations on ^{18}F-FDG PET/CT standardized uptake values," *J. Nucl. Med.*, vol. 46, pp. 424-428, 2005.

[20] M. Soret, S.L. Bacharach, and I. Buvat, "Partial-volume effect in PET tumor imaging," *J. Nucl. Med.*, vol. 48, pp. 932-945, 2007.

[21] K. Erlandsson, I. Buvat, P.H. Pretorius, B.A. Thomas, and B.F. Hutton, "A review of partial volume correction techniques for emission tomography and their aplications in neurology, cardiology and oncology," *Phys. Med. Biol.*, vol. 57, pp. 119-159, 2012.

Thinn Thinn Myint received B.Med.Tech (Medical Imaging) and B.Sc. (Physics) degrees from Medical Technology, Yangon and West University, Yangon in 2005 and 2011 respectively. In 2017, she studied master program in Radiological Technology in Mahidol University. Currently, she is a technical officer at Department of Nuclear Medicine, PET/CT and Cyclotron Center, Yangon General Hospital. Her research interests are nuclear medicine imaging, radiation protection and safety as well as medical image quality assessment.

Tawatchai Ekjeen received B.Sc. and M.Sc. degrees in Radiological Technology from Mahidol University, Thailand in 2006 and 2008, respectively. In 2014, he earned Ph.D. in Medical Technology from Mahidol University. Currently, he is a lecturer at Department of Radiological Technology, Faculty of Medical Technology, Mahidol University. His research interests are nuclear medicine imaging, Monte Carlo simulation in nuclear medicine, and medical image quality assessment.

Kanyalak Wiyaporn received B.Sc. and M.Sc. degrees in Radiological Technology from Mahidol University, Thailand in 2007 and 2009, respectively. In 2013, she earned Ph.D. in Medical Technology from Mahidol University. Currently, she is a lecturer at Department of Radiological Technology, Faculty of Medical Technology, Mahidol University. Her research interests are nuclear medicine imaging, Monte Carlo simulation in nuclear medicine, and tracer kinetic modeling in myocardial perfusion quantification using PET.

Anucha Chaichana received B.Sc. and M.Sc. degrees in Radiological Technology from Mahidol University, Thailand in 2012 and 2016, respectively. Currently, he is a teaching assistant at Department of Radiological Technology, Faculty of Medical Technology, Mahidol University. His research interests are nuclear medicine imaging, internal radiation dosimetry, and deep learning for medical image processing.

Yudthaphon Vichianin received his B.Sc. in Radiological Technology from Mahidol University, Thailand and M.S. in Information System from Hawai'i Pacific University, U.S.A. He received Ph.D. in Information and Communication Science from University of Hawai'i, Manoa, U.S.A. His research interests are computer simulation in radiological education, PACS, and software application in RT.

Ruentip Tipparoj received B.Sc. degree in Radiological Technology from Mahidol University, Thailand in 1998, and M.Sc. in Radiological Science from Faculty of Medicine Siriraj Hospital, Mahidol University, Thailand in 2008. She is a technologist at Division of Nuclear Medicine, Department of Radiology, Faculty of Medicine Siriraj Hospital, Mahidol University. Her research interests are nuclear medicine imaging and medical image quality assessment.

Thonnapong Thongpraparn received B.Sc. (Physics) degree from Srinakharinwirot University (Prasarnmit), Thailand in 1994. He earned master degree in Nuclear Engineering (Nuclear Technology) from Chulalongkorn University, Thailand in 1998. Currently, he has academic position as Assistant Professor. He also works as Lecturer and Medical Physicist at Division of Nuclear Medicine, Department of Radiology, Faculty of Medicine Siriraj hospital, Mahidol university. His research interests are nuclear medicine imaging, radiation protection and safety as well as medical image quality assessment.

Associate Professor Sunanta Chiewvit received doctor of medicine degree from Khon Kaen University, Thailand in 1990. She graduated nuclear medicine training from Mahidol University, Thailand in 1993. Currently, she is an associate professor at Department of Radiological, Faculty of Medicine, Mahidol University. Her research interests are nuclear medicine imaging and treatment.